

## DAMAGE SURVEY AND MAPPING OF THE 2006 CENTRAL JAVA EARTHQUAKE WITH ENHANCED USE OF SATELLITE IMAGES AND GPS

FUMIO YAMAZAKI

Department of Urban Environment Systems, Chiba University  
1-33 Yayoi-cho, Inage-ku, Chiba 263-8522, Japan.

MASASHI MATSUOKA

National Research Institute for Earth Science and Disaster Prevention (NIED)  
1-5-2 Kaigandori, Wakinohama, Chuo-ku, Kobe 651-0073, Japan.

### ABSTRACT

This paper highlights the recent applications of remote sensing technologies in post-disaster damage assessment, especially in the 2006 Central Java earthquake. After the Central Java earthquake, satellite images which captured the affected areas before and after the event were fully employed in field investigations and in damage mapping together with GPS data. Using the high-resolution optical satellite images, the areas of building damage were extracted based on pixel-based and object-based land cover classifications and their accuracy was compared with visual inspection results. Considering the results from the companion papers, the use of proper satellite imagery is suggested taking into account the area to cover, sensor type, spatial resolution, satellite's retake time etc., in post-disaster damage assessment.

### INTRODUCTION

In the recent few years, large-scale earthquakes and tsunamis brought tremendous damages to urban and rural areas in the world. It is also pointed out that rapid expansion of urban areas in developing countries has made the areas more vulnerable to various natural disasters. Thus, damage assessments before and after disasters have attracted significant attentions among researchers and practitioners of disaster management. Recent advancements in remote sensing and its application technologies made it possible to use remotely sensed imagery data for assessing vulnerability of an area and for capturing the distribution of damages due to disasters.

To obtain the pre- and post-event spatial information on built and natural environments, several methods exist, such as field survey, airborne remote sensing, and satellite remote sensing. Because of its capacity to cover a vast area in one acquisition time, satellite remote sensing has been a very powerful tool to monitor the condition of the earth surface. High-resolution satellite imagery, which has become available in the last few years, made satellite remote sensing more useful in disaster management since even the damage status of individual buildings and infrastructures can be identified without visiting the sites of disasters. The present authors have applied the images from QuickBird, the highest resolution commercial optical satellite, to obtain the damage status of individual buildings due to the 2003 Boumerdes, Algeria, earthquake (Yamazaki et al. 2004) and the 2004 Bam, Iran, earthquake (Yamazaki et al. 2005). The recent accumulation of pre-disaster images make post-disaster images more valuable since change (damage) detection can be carried out using them.

In this paper, the applications of satellite imagery to post-disaster damage assessment are demonstrated for the 27 May 2006 Central Java earthquake. The pre- and post-event satellite images are employed as base-maps for field damage survey together with GPS, and they are used in visual and automated damage detection.

## THE CENTRAL JAVA EARTHQUAKE AND FIELD SURVEY

A strong earthquake of magnitude 6.3 struck Java Island, Indonesia, on May 27, 2006 at 5:54 am local time. The epicenter was located at 7.962°S, 110.458°E, about 25 km south-southeast of Yogyakarta with a fairly shallow focal depth, about 10 km (Figure 1). Due to this earthquake, almost 6,000 people were killed and about 38,000 people were injured. About 140,000 houses were collapsed and about 190,000 houses were heavily damaged (USGS 2006, UNOSAT 2006).

After the earthquake, various international teams conducted damage surveys of the affected area. As one of sub-teams of the research group supported by the Ministry of Education, Science, Sports and Culture (MEXT), Japanese Government, Grant-in-Aid for Special Purposes (No.1890001, 2006), the present authors visited the affected area from 26 to 30 June, 2006. The main objective of our sub-team was to gather geo-referenced ground truth data, which can be used to validate the damage detection results from satellite images.

Figure 2 shows the route of the field survey. The camera icons on the map show the locations where we took geo-referenced digital photos.

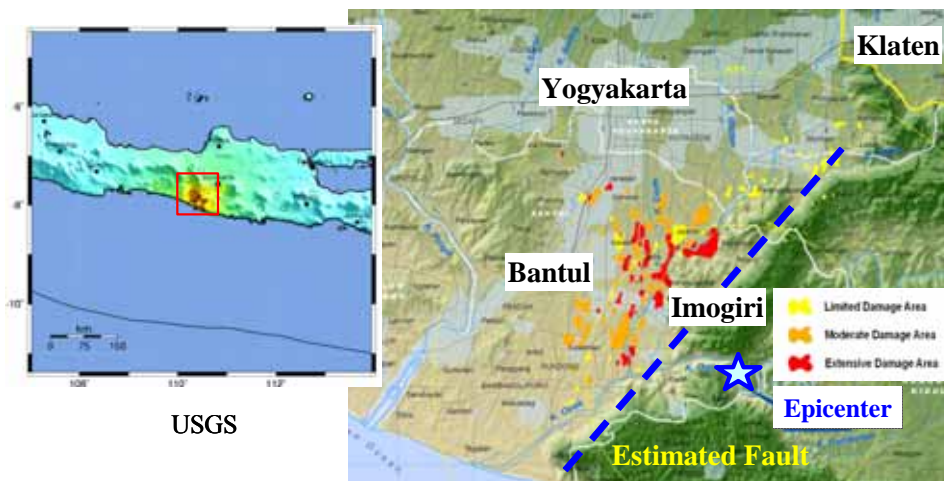


Figure 1. Epicenter of the 2006 Central Java earthquake (USGS 2006) and preliminary damage assessment map produced by UNOSAT (2006) on May 31, 2006.

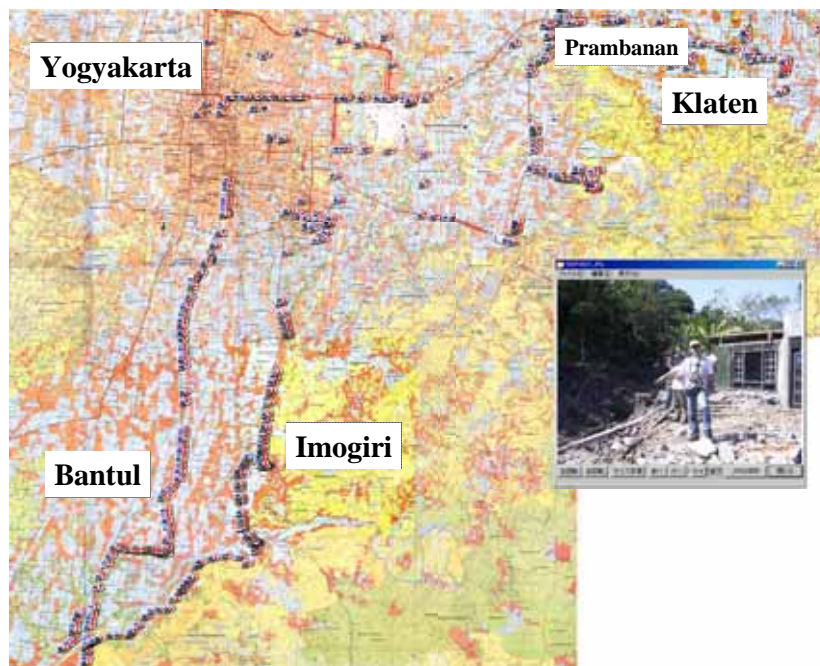


Figure 2. Field survey route by the authors. Camera icons show the locations of GPS synchronized photo shooting.

Figure 3 shows typical damages observed in the field. Figure 3(a) is collapsed brick-masonry houses in a rural area. This type of total collapses of walls and roofs were seen everywhere and considered to be responsible for many casualties in this earthquake in spite of its small magnitude. Figure 3(b) shows a collapsed reinforced-concrete school building. Such severe damages to engineered buildings were seen only at limited locations. Figure 3(c) shows a large-scale landslide observed in a mountainous area. In Prambanan World Heritage, the largest Hindu temple compound in Indonesia, many big stones were fallen down from the towers as shown in Figure 3(d). The site has been closed to tourists since the earthquake and it was reported that the restoration may take a few years.



Figure 3. Typical damages seen in the field survey: (a) collapsed brick-masonry houses in a rural area, (b) a collapsed reinforced-concrete school building, (c) a large-scale landslide observed in a mountainous area, (d) stones fallen down from the towers in Prambanan temple compound.

#### DAMAGE DETECTION USING QUICKBIRD IMAGE

QuickBird has 0.6 m resolution in panchromatic mode and 2.4 m resolution in multispectral mode with 4 bands: blue, green, red, and near-infrared. A pan-sharpened image of 0.6 m resolution can be produced through combining a panchromatic image and a corresponding multispectral image. After the Java Earthquake, QuickBird captured a clear image of the affected areas on June 13, 2006. The image includes Imogiri, one of the most severely affected areas in this earthquake. For the area, a pre-event image captured on July 11, 2003 also exists. Thus a part of these images, shown in Figure 4, were used in this study.

First, a pixel-based classification was carried out based on the maximum likelihood method, the most common supervised classification method, using 8-bit four bands data. The following 8 classes: black-roof, gray-roof, red-roof, white-roof buildings, road, soil, vegetation, and shadow, were assigned for the pre-event image as the training data. For the post-event image, 7 classes: black-roof, gray-roof, red-roof buildings, debris, road, vegetation, and shadow, were assigned. White-roof building and soil classes were not used for the post-event image because they look close to the debris class and it was difficult to select their training data. The building areas obtained by the pixel-based classification are shown in Figure 5(a) and Figure 6(a). In these figures, the buildings with different roof-color are shown in the same color for easier understanding.

Next, an object-based classification was conducted using e-Cognition software. Image segmentation was carried out as the first step to make “objects” using the pre-event and post-event images. In e-Cognition, the segmentation process is determined by 5 parameters: *Layer Weight*,

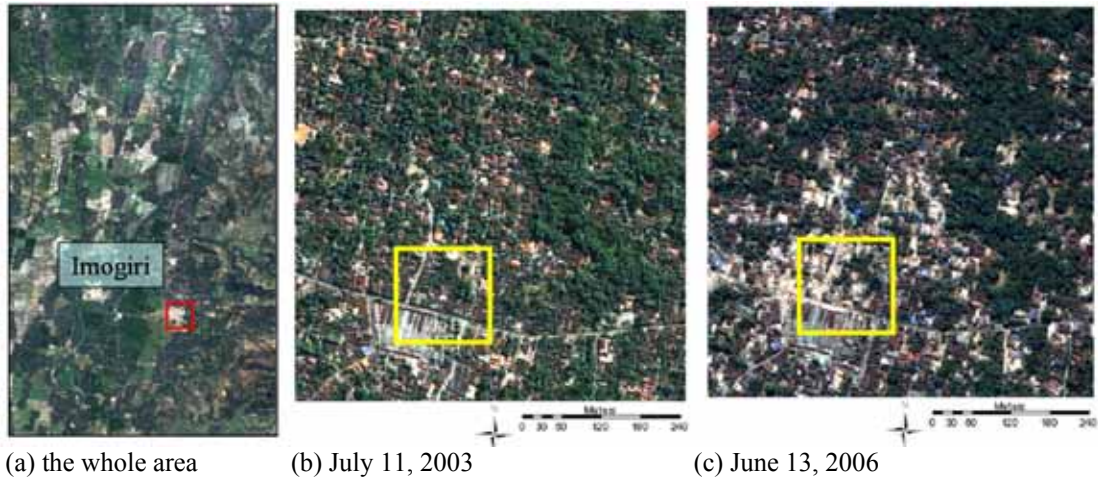
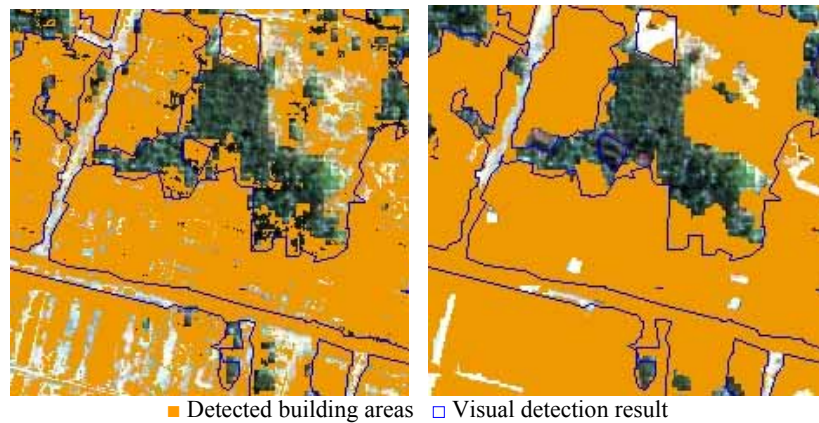


Figure 4. (a) Pan-sharpened natural color QuickBird images of Imogiri area, (b) is the pre-event image and (c) is the post-event image used in this study.

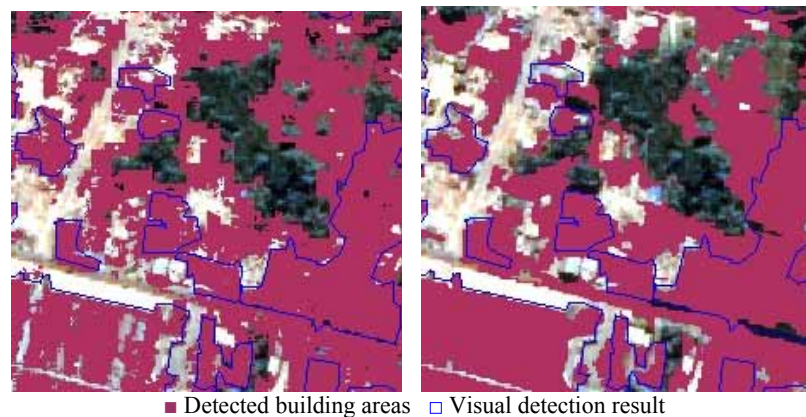


(a) Pixel-based classification (b) Object-based classification

Figure 5. Part of the pre-event image (yellow square in Figure 4 (b)) and the result of land cover classifications.

*Compact Weight*, *Smooth Weight*, *Shape Factor*, and *Scale Parameter* (Baatz et al. 2004). The most important parameter is the *Scale Parameter*, which determines the object size. The *Shape Factor* is to determine the importance level of spectral heterogeneity or shape heterogeneity in segmentation. When the shape factor moves toward 0, the spectral heterogeneity is more concerned. On the contrary, if it moves toward 0.9, the shape heterogeneity is more concerned. In further details, the spectral heterogeneity is decided by *Layer Weight*, which gives the weight for each band. The shape heterogeneity is decided by *Compact Weight* and *Smooth Weight*. The bigger the Compact Weight is, the segmented objects are in a more compact shape. Alternatively, the bigger the Smooth Weight is, the segmented objects are in a more smooth shape.

Starting from pixels, segmentation runs the merge between two objects and is terminated when an assigned condition is reached. This condition is defined based on the fusion value  $f$ , which measures the changes when merging and decided by the Layer Weight, Compact Weight, Smooth Weight, and Shape Factor. If  $f$  equals to or becomes bigger than the squared Scale Parameter, the condition is reached. Although it is difficult to decide the appropriate parameters values suitable to all land cover classes, the user can decide the suitable values to a few focused classes, e.g. building, road.



(a) Pixel-based classification      (b) Object-based classification

Figure 6. Part of the post-event image (yellow square in Figure 4 (c)) and the result of land cover classifications.

The appropriate parameters for buildings were used in this study and the image segmentation was conducted for the pre-event and post-event images. Then, the samples for all the classes were selected as the same areas in the pixel-based classification. The objects' mean values of blue, green, red, and near-infrared were used as the indices of classification and the nearest neighbor classification method was employed.

The results from the object-based classification for the pre-event and post-event images are shown in Figures 5(b) and 6(b), respectively. Comparing the results from the pixel-based and object-based classifications with that by visual inspection, salt-and-paper noises are seen in the pixel-based classification. Hence, it may be concluded that in this high resolution and the sizes of the target objects, the better result can be acquired by object-based classification. But in object-based classification, some road and shadow areas were misclassified to building classes because their spectral values of the sample area are similar to those of building classes. Hence even object-based classification, some classes like these are needed to remove in advance using object feature indices, e.g. length, or spatial relationships.

## CONCLUSIONS

The recent applications of remote sensing technologies in post-disaster damage assessment were highlighted using the satellite imagery obtained in the 27 May 2006 Central Java earthquake, as a typical example. After the Central Java earthquake, high-resolution optical satellite images were fully employed to extract the areas of severe building damage. In our field investigation, satellite images were used as base-maps together with GPS. Comparing the pre-and post-event QuickBird images, the areas of severe building damage were extracted based on pixel-based and object-based classifications and their accuracy was compared with visual inspection results.

In summary, considering the results from the companion papers in this workshop, satellite images can be used efficiently in post-disaster damage assessment if they are selected properly in terms of sensor type (optical or SAR), spatial resolution, satellite's retake time, and the availability of pre-event images and digital maps, etc.

## ACKNOWLEDGEMENT

Some research outputs introduced in this paper have been produced by Dr. Hiroyuki Miura of Tokyo Institute of Technology and Dr. Yoshihisa Maruyama and Mr. Kazuki. Matsumoto of Chiba University. Their contributions are deeply appreciated.

## REFERENCES

- Baatz, M., Benz, U., et al. (2004). *e-Cognition user guide 4*, Definiens Imaging, 76-78.
- UNOSAT (2006). Indonesia Maps, <http://unosat.web.cern.ch/unosat/asp/>.
- USGS (2006) URL: <http://earthquake.usgs.gov/eqcenter/eqinthenews/2006/usneb6/>
- Yamazaki, F., Kouchi, K., Matsuoka, M., Kohiyama, M., and Muraoka, N. (2004). "Damage Detection from high-resolution satellite images for the 2003 Boumerdes, Algeria Earthquake", *Proceedings of the 13th WCEE*, CD-ROM, Paper No. 2595.
- Yamazaki, F., Yano, Y., and Matsuoka, M. (2005). "Visual damage interpretation of buildings in Bam city using QuickBird images", *Earthquake Spectra*, Vol. 21, No. S1, S329-S336.